

Diffuse Interstellar Bands in single clouds: new families and constraints on the carriers

J. Cami^{1,2,3}, P. Sonnentrucker^{4,5}, P. Ehrenfreund^{3,6}, and B.H. Foing^{4,6}

¹ SRON Groningen, P.O. Box 800, 9700 AV Groningen, The Netherlands

² Astronomical Inst. “Anton Pannekoek”, Univ. of Amsterdam, Kruislaan 403, 1098 SJ Amsterdam, The Netherlands

³ Leiden Observatory, P.O. Box 9513, 2300 RA Leiden, The Netherlands

⁴ Solar System Division, ESA Space Science Department, ESTEC/SO, 2200 AG Noordwijk, The Netherlands

⁵ Observatoire de Strasbourg, 11 rue de l’Universite, F-67000 Strasbourg, France

⁶ Institut d’Astrophysique Spatiale, CNRS, Bat 121, Campus d’Orsay, F-91405 Orsay, France

Received 27 March 1997 / Accepted 22 May 1997

Abstract. We present a survey of diffuse interstellar bands (DIBs) in single clouds. High resolution and high S/N observations of DIBs towards lines of sight representing very different environments allow to investigate mutual correlations in a large consistent sample of DIBs. The classification of DIBs into families is reviewed and refined according to these results. We find that the selected 44 DIBs are due to different carriers. Two isolated families of DIBs ($\lambda 5797$ et al., $\lambda 4501$ et al.) are found, which are mutually slightly anticorrelated. The behaviour of DIBs with respect to the local UV field is investigated using hydrogen column densities to estimate the strength of the UV field, resulting in the hypothesis that most of the DIB carriers are molecules sensitive to photo-ionization. With this interpretation, the apparent division of interstellar clouds into ζ , σ and *Orion* types can be understood as a sequence in strength of the UV field. Differences in strength of the UV field between different lines-of-sight are due to the so-called “skin-effect”, the effective shielding of UV radiation by the outer layers of interstellar clouds.

Key words: ISM: molecules – ISM: dust – molecular data

1. Introduction

Almost every paper about Diffuse Interstellar Bands (DIBs) starts with stating that the identification of the DIB carriers is one of the longest standing unsolved problems in spectroscopy. The identification of the DIB carriers is indeed an important problem in modern astronomy and a recent review on this topic presented by Herbig (1995) showed the enormous progress of this field in the recent years.

Send offprint requests to: P. Ehrenfreund

Over 200 well defined absorption bands in the visible range from 4430 Å extending to the near infrared are observed in different regions of the interstellar medium. The strongest band at 4431 Å was already observed by Cannon between 1911 and 1919 in the spectrum of a heavily reddened B supergiant (Code 1958). The interstellar nature of these absorption bands was first suggested by Merrill (1934) from the correlation of band intensities with the color excess and the constant wavelength of the features in different lines of sight.

A wide variety of possible carriers like small dust grains, gas phase molecules or impurities embedded in grains have been proposed (see Herbig 1995 for a review) and several attempts have been made to identify the DIB carriers by comparing DIB spectra with laboratory measurements. So far this resulted only in the positive identification of two DIBs with C_{60}^+ (Foing & Ehrenfreund 1994, 1997) while dedicated searches for other molecules like coronene and ovalene led to small upper limits (Ehrenfreund et al. 1995). Important possible carrier molecules are PAHs which show promising similarities with DIBs (see Salama et al. 1996 for a review). These authors propose to correlate the known DIB spectrum with 150-200 stable PAH ions, proposing a 1 DIB - 1 PAH hypothesis. The numerous possible DIB carriers proposed so far imply that DIB spectra should be compared with a huge amount of laboratory data from difficult and time consuming experiments. Hence, observational studies have tried to eliminate classes of proposed carriers to simplify the identification.

An important breakthrough has come from the comparison of DIB line profiles with theoretical calculations of rotational contours for PAHs and fullerenes. Rotational constants derived from the peak separations in three DIBs showing substructures ($\lambda 5797$, 6379 and 6613) point to large molecular carriers (such as 30 C rings, 40-50 C PAHs or fullerene compounds, see Ehrenfreund & Foing 1996). A good profile fit with 14-30 C-rings was obtained by Kerr et al. (1996).

The strongly variable DIB strength in different lines of sight has led to attempts to group DIBs into families that show similar variations from one line-of-sight to another, albeit with contradictory results (Chlewicki et al. 1986; Krelowski & Walker 1987; Josafatsson & Snow 1987; Krelowski & Westerlund 1988). However, this has not yet led to firm constraints on the DIB carriers.

As the DIBs are intrinsically weak features, observations of DIBs have often been done towards heavily reddened stars, where a line-of-sight samples several intervening clouds. This makes the interpretation of the data less sensitive and more difficult, as it is not clear which physical parameters influence the DIB strength. Only since the advent of sensitive CCD cameras, it is possible to obtain accurate measurements of DIB strengths towards low reddened stars mainly obscured by only one intervening cloud, the so-called single cloud stars. This study presents results obtained from DIB observations towards 13 single cloud stars where special attention has been made to include interstellar clouds representing very different environments.

2. Observations

2.1. Data acquisition

Observations were carried out at the *Observatoire de Haute Provence* (OHP) in July and November 1995. We used the 1.93m telescope equipped with the ELODIE fiber-fed echelle spectrograph, covering the wavelength range from 3906 to 6811 Å with a resolution of ~ 42000 (Baranne et al. 1996). Table 1 lists basic stellar data, the obtained S/N and other data used further in this paper for the program stars.

2.2. Measurements

We used the DIB-survey of Jenniskens & Désert (1994, JD94 hereafter) to identify DIBs that fall in the observed wavelength range. This list has more DIBs than another list by Herbig (1975, 1995) but does also show differences in DIB definition. Features listed by Herbig as one DIB are sometimes decomposed into different components by JD94 and differences in the width and strength of DIBs exist, which suggests caution in using the list of JD94.

Equivalent widths are measured by integrating over the line profile and calculating

$$W = \sum_i \left(1 - \frac{I_i}{I_i^c}\right) \Delta\lambda$$

where I^c is the continuum baseline, I is the observed intensity and the sum runs over the pixel indices in the feature ($\Delta\lambda$ is the pixel width). Random errors on the equivalent widths including noise on integration and continuum positioning are typically

$$\Delta W = rms \sqrt{2\Delta\lambda FWHM}$$

where rms is the relative root mean square noise per pixel. For a typical narrow DIB with a FWHM of 1 Å and a typical S/N of 300, this error is typically ~ 2 mÅ. Clearly this is an

optimistic estimate; systematic errors can be expected to be higher, in particular for weak or very broad DIBs.

In spectral ranges severely contaminated by atmospheric lines, the spectrum of the program star is divided by that of a non-reddened standard star with very low reddening observed at the same airmass which removes (or at least reduces) the atmospheric lines. Equivalent widths are measured in the telluric corrected spectrum, which generally has a lower S/N; hence the error on the equivalent widths is larger in telluric corrected spectra.

2.3. Description of the star sample

The program stars as listed in Table 1 represent very different environments (see Sect. 4) located in three major cloud complexes.

HD145502, HD144217 and HD149757 are part of the Sco OB2 association located towards the large Sco-Oph complex in the region of ρ Oph. The distance to the complex is about 165 pc, so the effects of intervening interstellar material are small. The complex shows a large variation in density within the cloud. HD144217 and HD145502 are two B stars in Upper Scorpius, while HD149757 is part of Ophiuchus itself and is located more towards the center of the complex.

One of the nearest OB associations is Per OB2. The association is seen in a sky region covered with a very extended molecular cloud, easily observable in molecular radio lines. Krelowski et al. (1996) note that the region contains both σ and ζ clouds (see discussion in Sect. 4) as well as some intermediate types. They conclude that the complex consists in fact of two partially overlapping clouds differing strongly in their optical properties. The five stars selected in this region (HD23180, HD24398, HD22951, HD24760, HD24912) are distributed over this complex and the different cloud types.

Finally, there are 5 stars located in the constellation of Orion. HD37020 and HD37022 are two of the Trapezium stars in the Orion Nebula. HD36486 and HD38771 are located near the edges of the HII complex while HD36861 lies further away. Most, if not all, of the reddening in these lines of sight is due to matter that is part of the Orion giant molecular complex (GMC). Because Orion is nearby (500 pc) and far below the galactic plane (180 pc), there is little foreground reddening.

2.4. The final DIB-sample

In order to have a consistent data set and DIB definition, we measured the well-studied star HD183143 and compared our measurements with the results found in JD94. The two sets of data are generally in agreement with each other. Small but significant differences (~ 5 -10%) were found for DIBs blended with stellar lines and with other DIBs. These differences can be explained by the higher resolution of our data which makes it easier to discern and accurately measure the separate components. Larger differences (~ 10 -20%) occur for DIBs that were measured in telluric corrected spectra where we used better standards than JD94, which points to a non-negligible contribution

Table 1. The program stars. The left part of the Table lists basic stellar data and S/N, the right part hydrogen data taken from Savage et al. (1977) where $f = \frac{2N(\text{H}_2)}{N(\text{HI})+2N(\text{H}_2)}$ and T_{01} is the kinetic temperature determined from the $J = 0$ to $J = 1$ rotational transition in H_2 . HD183143 has only been used for average interstellar medium comparison.

HD	Name	Sp. T.	V	E_{B-V} (mag.)	S/N	log	log	log	log f	T_{01}
						N(H_2) [cm^{-2}]	N(HI) [cm^{-2}]	N(HI+ H_2) [cm^{-2}]		
145502	ν Sco	B2Vp	4.01	0.27	260	19.89	21.15	21.19	-1.00	90
144217	β^1 Sco	B0.5III	2.62	0.20	298	19.83	21.09	21.14	-1.01	88
149757	ζ Oph	O9.5 Vn	2.56	0.32	301	20.65	20.72	21.15	-0.20	54
23180	σ Per	B1III	3.83	0.30	270	20.61	20.90	21.21	-0.30	48
24398	ζ Per	B1Ib	2.85	0.33	378	20.67	20.81	21.20	-0.23	57
22951	40 Per	B1 IV	4.97	0.23	317	20.46	21.04	21.23	-0.46	63
24760	ϵ Per	B0.5 III	2.96	0.10	290	19.53	20.40	20.50	-0.67	81
24912	ξ Per	O7.5 IIIInf	4.04	0.29	304	20.53	21.11	21.30	-0.46	61
37020	θ^1 Ori A	O7	6.37	0.4	190	-	-	-	-	-
37022	θ^1 Ori C	O6	5.13	0.31	350	<17.55	21.04	21.04	<-3.22	-
36486	δ Ori	O9.5 II	2.23	0.07	417	14.68	20.23	20.23	-5.25	1625
36861	λ Ori	O8 IIIf	3.66	0.12	340	19.11	20.78	20.80	-1.38	45
38771	κ Ori	B0.5 Ia	2.06	0.07	400	15.68	20.52	20.52	-4.54	156
183143		B7Iae	6.9	1.28						

to the equivalent width for some DIBs in stars having a very low E_{B-V} that were used as standard stars.

Next we measured the DIBs in the program stars. For various reasons however, we reduced the number of DIBs in the sample. First, as DIBs are generally weak features in the program stars, it is very difficult to set the continuum baseline accurately for very broad DIBs. Where we encountered severe difficulties doing so (e.g. at the edges of adjacent orders), we excluded the DIB from our final sample. Second, DIBs contaminated by stellar lines were also rejected when the stellar component was not clearly discernible; in other cases the stellar contribution to the equivalent width was measured separately and subtracted. Finally, we did not include DIBs measured in the telluric corrected spectra. As mentioned above, using a standard with very low (or perhaps even 0.00) reddening is no guarantee for absence of DIBs in these spectra. As we do not have any *a priori* knowledge of the DIB strengths in those stars, we preferred not to include these DIBs. Our final sample thus includes 44 DIBs (see Table 2).

The equivalent widths measured are furthermore normalized to E_{B-V} , which possibly introduces another small error.

3. Families of DIBs?

3.1. Why single clouds?

The large number of known DIBs has raised the obvious question whether or not several DIBs could be originating from the same carrier, contrary to the 1 DIB - 1 carrier hypothesis. It was argued that DIBs originating from the same carrier should behave exactly the same in different environments and hence the strengths of these DIBs in different lines-of-sight should be perfectly correlated. Based on this idea and on the correlation of DIB strength with E_{B-V} different attempts have been made to classify DIBs into families (Chlewicki et al., 1986; Krelowski

& Walker, 1987; Josafatsson & Snow, 1987) but no good agreement was found between the different classifications.

The confusion thus arising is caused by the fact that these studies only include a very small number of DIBs and, more important, often include DIBs measured towards heavily reddened stars. Where a line-of-sight samples several intervening clouds, the total DIB strength measured is composed of the contributions from every cloud, and averages out the effect of local physical differences. However, the physical conditions that define the DIB strength may well be quite different for the individual clouds. As a consequence, the resulting DIB strength is hard to interpret which makes the search for DIBs originating from the same carrier difficult, if not impossible. It is clear that correlations pointing to similarities on the level of the DIB carriers can only be found from *single cloud* observations. On the other hand, the most reliable correlations can be expected for observations that include a wide range of environments: only DIBs that behave in the same way in *every* environment can originate from the same carrier.

The previous arguments provide us with a justification for this work: the program stars listed in Table 1 can be considered as - in first approximation - single clouds. The interstellar Na and Ca lines towards these lines of sight show only one major component; the amount of interstellar matter contained in eventual secondary components is at least an order of magnitude smaller. Moreover, as will be shown in Sect. 4, these lines of sight sample clouds showing rather drastic differences in physical properties.

This study, based on DIB measurements in single clouds covering different environments, thus offers for the first time a good possibility to investigate both possible DIB correlations and the nature of the DIB carriers.

3.2. Mutual DIB correlations: errors, bias and confidence.

Correlation coefficients offer a good mathematical tool to quantify similarities between two sets of observations. The interpre-

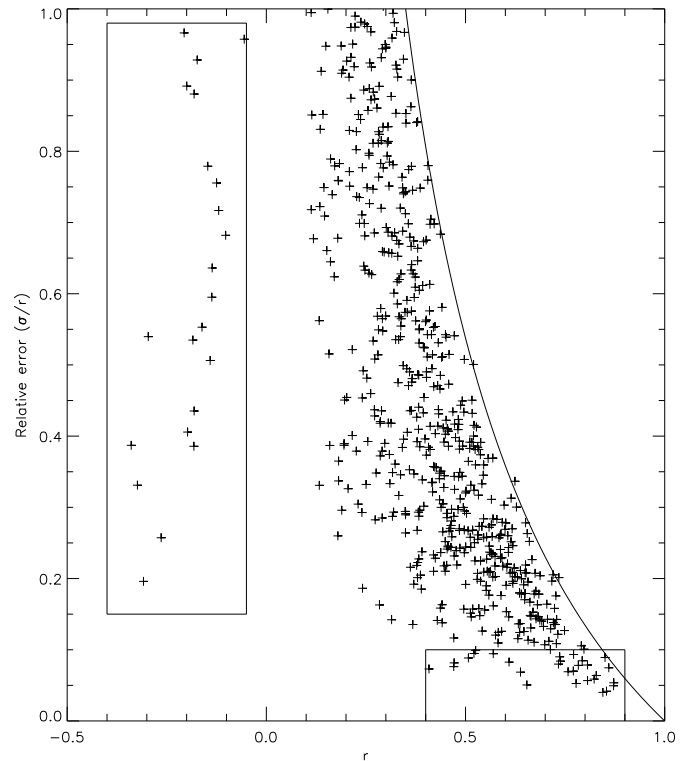
Table 2. Statistically averaged autocorrelation coefficients r and the standard deviation σ on the average for the DIBs in our sample.

λ DIB	r	σ	λ DIB	r	σ
4501.80	0.97	0.02	6089.80	0.52	0.26
4726.59	0.75	0.20	6194.87	0.22	0.46
4727.06	0.94	0.03	6196.19	0.86	0.09
4762.57	0.85	0.10	6203.19	0.96	0.02
4780.09	0.96	0.01	6204.33	0.92	0.03
4880.35	0.54	0.32	6234.27	0.98	0.01
4963.96	0.68	0.21	6270.06	0.92	0.08
5404.56	0.74	0.19	6270.36	0.99	0.01
5487.49	0.93	0.03	6308.93	0.68	0.14
5494.14	0.85	0.10	6353.49	0.90	0.07
5508.35	0.98	0.02	6367.22	0.51	0.26
5544.97	0.48	0.23	6376.07	0.76	0.16
5747.81	0.99	0.00	6379.27	0.98	0.01
5776.08	0.86	0.11	6397.39	0.82	0.15
5780.59	1.00	0.00	6425.72	0.81	0.06
5789.06	0.94	0.03	6491.88	0.13	0.39
5795.23	0.97	0.01	6494.17	0.68	0.15
5797.11	0.98	0.01	6520.70	0.39	0.22
5809.12	0.61	0.32	6613.72	0.99	0.00
5809.96	0.11	0.43	6770.05	0.32	0.35
5844.19	0.87	0.07	6792.45	0.91	0.05
5849.78	0.98	0.01	6811.44	0.85	0.08

tation of this one single number however depends on the kind of similarities searched for. The obvious question in our case to remain answered before classifying the DIBs is “what correlation coefficient is expected for DIBs originating from the same carrier?”. The answer is less than obvious.

Assuming that the DIB carriers are all kinds of molecules, the strength of a given DIB is determined by the fundamental level population. The ratio of two absorption lines originating from the same lower level in the same molecule would be constant in every environment, and thus lead to a correlation coefficient of 1.00. We will now assess the role of the errors on the measurements. Due to the fact that two measurements are never the same, two sets of observations of the same DIB in different environments yield a correlation coefficient lower than unity. To have an idea about the influence of measuring errors on the mutual correlations, we performed the following Monte Carlo experiment. For each DIB we produced two sets of observations by taking the series of equivalent width measurements in our program stars and adding random Gaussian noise with the same *rms* as the estimated errors on the measurements. Next we calculated the correlation coefficient between those two sets. This procedure was repeated 100 times, after which we averaged those 100 numbers and calculated the standard deviation σ on the derived average correlation coefficient r .

From Table 2 it is clear that those errors can play a very important role, introducing a systematic “decorrelation bias” of 1.8σ in the autocorrelation. Only calculating a correlation coefficient does not give us information about the reliability of the correlation.

**Fig. 1.** Relative errors on the correlation coefficients as a function of the correlation coefficient r . The hyperbolic curve on the right indicates the envelope expected for perfect correlations based on the observed noise-induced bias in the autocorrelation. Different domains are distinguished of well-correlated, moderately correlated and slightly anticorrelated DIB pairs, whose interpretation is discussed in the text.

We proceeded in the same way to calculate the mutual correlation coefficients. For each two DIBs considered, we added normal-distributed noise with the same *rms* as the errors on the individual measurements and we calculated a statistically averaged correlation coefficient and the standard deviation on this average. This gives a good idea about the reliability of the correlation coefficient.

That the errors on the measurements can drastically influence the reliability of the correlations, can be seen in Fig. 1. Note that reducing the errors on the measurements will generally not only reduce the error on the correlation coefficients but also increase the value of the correlation coefficient for DIBs that do correlate well (due to the bias mentioned in Table 2).

We now get back to the classification of DIBs into families. Keypoint is the assumption that DIBs originating from the same carrier should have the same behaviour in different environments. Therefore we have to look for DIBs whose strengths in those environments correlate perfectly with each other. To have reliable results, we have to put a limit on the error on the correlation coefficient.

3.3. Interpretation of the mutual correlations.

We distinguish different DIB groups, according to the values of the correlations and their errors as indicated in Fig. 1.

(a) DIBs which are possibly perfectly correlated (indicative of the same carrier) whose debiased mutual correlation ($r + 1.86\sigma$) overlaps confidently within the error bars with a correlation >0.9 . We could not find in our sample such perfectly correlating DIBs with a confidence higher than 60%.

(b) DIBs that would arise from carriers of similar physical nature whose correlation is in the range 0.7 - 0.9 with sufficient confidence. In Fig. 1, our criteria show we have to focus on the lower right part of the plot, where a tail groups 19 datapoints with a correlation coefficient $r > 0.70$ and the relative error $\frac{\sigma}{r} < 0.1$. These correlations are listed in Table 3.

Although only a small fraction of the available data seems reliable enough for our purposes, Table 3 gives already important clues about possible similarities between some DIBs.

The $\lambda 6270.06$ and $\lambda 6270.36$ DIBs do correlate well with each other. As the former is much narrower than the latter, this suggests that the $\lambda 6270.06$ DIB is in fact a substructure of the $\lambda 6270.36$ DIB and thus form one DIB. We will therefore not consider these two DIBs as one family, but rather say that the DIB-definition used from JD94 was not correct for these DIBs.

The other correlations in Table 3 show two reliably isolated families of DIBs:

- The $\lambda\lambda 5797, 6379$ and 6613 DIBs
- The $\lambda\lambda 4501, 5789, 6353$ and 6792 DIBs

All members of both families do correlate with all the other members in the same family. In the case of the $\lambda 5797$ family, there are no other DIBs that correlate with any of the DIBs in the family, but in the case of the $\lambda 4501$ family, some DIBs correlate with one of the DIBs in the family; those DIBs are however no “close” members as they don’t correlate with the other DIBs in the family.

There are two more couples of DIBs, $\lambda\lambda 5780, 6203$ and $\lambda\lambda 5508, 5849$, that correlate well with each other but not with any other DIB.

There is other evidence that the members of the $\lambda 5797$ family may have a similar carrier. Comparison with theoretical contour calculations have shown that the line profiles and line widths of the three DIBs in this family are compatible with rotational contours of fullerene compounds, large carbon rings or PAHs (see Ehrenfreund & Foing 1996). The DIBs in the $\lambda 4501$ family are all very weak, hence a line profile study has not been made yet, but they do have comparable widths (from 1.1 - 2.5 Å). In addition, there are a few DIBs ($\lambda\lambda 5508, 5849, 5776, 5487$) that do not correlate as well with all members of this family.

(c) Well-measured DIBs that have reliable correlation coefficients (error $< 10\%$) indicating only a moderate correlation ($0.4 < r < 0.7$). We note that the correlation coefficient between $\lambda 5780$ and $\lambda 5797$ is even lower, $r = 0.28 \pm 0.04$.

(d) DIBs which are slightly anticorrelated. There are only a few pairs of those. It is interesting to note that representatives of the previously defined isolated families are slightly

Table 3. Mutual correlations and errors for different categories of DIBs: well-correlated (top), moderately correlated (middle) and slightly anticorrelated (bottom).

DIB1	DIB2	r	σ
4501.80	5508.35	0.81	0.05
4501.80	5789.06	0.77	0.07
4501.80	6353.49	0.83	0.05
4780.09	5487.49	0.73	0.06
4780.09	5747.81	0.74	0.06
5487.49	5747.81	0.87	0.05
5487.49	6353.49	0.81	0.06
5508.35	5849.78	0.87	0.04
5508.35	6353.49	0.74	0.07
5747.81	5795.23	0.77	0.05
5776.08	5789.06	0.86	0.06
5780.59	6203.19	0.76	0.05
5789.06	6353.49	0.79	0.07
5789.06	6792.45	0.78	0.06
5797.11	6379.27	0.85	0.04
5797.11	6613.72	0.78	0.04
6270.06	6270.36	0.82	0.05
6353.49	6792.45	0.85	0.08
6379.27	6613.72	0.84	0.03
4501.80	5747.81	0.57	0.05
4780.09	5780.59	0.64	0.04
5487.49	5780.59	0.52	0.05
5747.81	5780.59	0.41	0.03
5780.59	6270.06	0.53	0.05
5780.59	6270.36	0.47	0.04
5780.59	6379.27	0.47	0.04
5780.59	6613.72	0.65	0.03
6203.19	6379.27	0.51	0.04
6203.19	6613.72	0.61	0.05
4501.80	6613.72	-0.14	0.07
4726.59	5776.08	-0.21	0.20
4726.59	6204.33	-0.17	0.16
4726.59	6494.17	-0.20	0.18
4727.06	6494.17	-0.18	0.16
5747.81	6613.72	-0.06	0.05
5776.08	5797.11	-0.16	0.09
5789.06	5797.11	-0.14	0.08
5797.11	6204.33	-0.26	0.07
5797.11	6234.27	-0.20	0.08
5797.11	6353.49	-0.18	0.08
5797.11	6494.17	-0.34	0.13
5797.11	6811.44	-0.15	0.11
6234.27	6379.27	-0.10	0.07
6234.27	6613.72	-0.18	0.07
6353.49	6379.27	-0.12	0.09
6353.49	6613.72	-0.31	0.06
6379.27	6494.17	-0.32	0.11
6379.27	6811.44	-0.14	0.09
6494.17	6613.72	-0.30	0.16
6613.72	6792.45	-0.12	0.09
6613.72	6811.44	-0.18	0.10

anticorrelated, with $\lambda 4501, 5776, 5789, 6353$ behaving opposite to $\lambda 6613, 5797$ and 6379 . Another class of DIBs $\lambda 6203, 6234, 6494, 6811$ seems slightly anticorrelated with $\lambda 5797$ et al. but do not form a closed family themselves.

(e) The fact that we do not find perfectly anticorrelated DIBs and also that there is a much larger number of positive correlations indicates that within our DIB sample other parameters favour a positive correlation coefficient.

4. The nature of the DIB-carriers

4.1. The ionization hypothesis

Single cloud DIB observations offer the possibility to investigate how DIBs respond to their environment, as the line-of-sight conditions are dominated by a single intervening cloud and can hence be described by other line-of-sight parameters (UV-field, electronic and hydrogen densities, etc.).

To have an idea about the strength of the local UV field for our different lines of sight, we use column densities for HI and H₂ as given by Savage et al. (1977, see Table 1). As H₂ dissociates under influence of UV radiation, the relative HI column density (that is $\frac{HI}{HI+2H_2}$) gives a good first approximation of the strength of the local UV field.

Fig. 2 shows the normalized equivalent width of the $\lambda 5780$ DIB as a function of relative HI column density. We show this strong DIB because the errors on the measurements are very small and because it illustrates very well what happens for some of the other DIBs.

The general behaviour is that for low values of HI/(HI+H₂) this DIB is weak. Increasing the value of HI/(HI+H₂) yields increasing DIB strengths until a maximum is reached after which the DIB strengths decrease with increasing HI/(HI+H₂). Assuming that this ratio is indeed a good parameter to estimate the strength of the local UV-field, this can be explained as a kind of “ionization” behaviour: if the DIB carriers are in some ionization stage n , we would expect weak DIBs for weak UV fields as most molecules are at stage $n - 1$. At moderate strength of the UV field stage n dominates which causes the DIB strength to increase too. But when the molecules reach the ionization stage $n + 1$, the DIB strength logically decreases again. Note that in the case of large molecules (smaller than 50 C-atoms) second ionization may lead to destruction or dehydrogenation of the molecule. At the right part of Fig. 2, where the HI/(HI+H₂) ratio reaches unity, it is clear that also HII column densities should be taken into account to distinguish well between the Orion stars.

There are however big differences between the curves of DIBs that do not correlate. Fig. 2 illustrates this for the $\lambda 5780$ and the $\lambda 5797$ DIBs whose mutual correlation coefficient is only $r = 0.28 \pm 0.04$. Where the $\lambda 5780$ DIB seems to reach the maximum only for strong UV radiation, the $\lambda 5797$ DIB seems to reach this maximum rather early and declines slowly afterwards. This is consistent with the ionization potential estimated for the carriers of the $\lambda 5797$ to be lower than for $\lambda 5780$ based on variations modeled in τ Per and Orion lines-of-sight (Son-

nenrucker et al. 1997). From this we can conclude that DIBs that correlate well with each other seem to have similar ionization potentials while DIBs that do not correlate with each other have very different ionization and recombination properties. The $\lambda 6353$ variation is further different with an increase only in high UV conditions, indicating an even higher ionization potential than the $\lambda 5780$ DIB.

The behaviour described above is seen for almost all DIBs; in some cases the errors on the measurements do not allow to draw definite conclusions.

Fig. 2 shows however that the parameter used, the relative HI column density, can only be a first approximation to describe the parameters that influence the DIB strength. Moreover it can be seen from the Figures that the rise and decline is not always evident as there are small but significant deviations from this behaviour that are larger than the measurement inaccuracies. This can be due to the fact that there are other parameters than the strength of the UV field that determine the strength of the DIBs or that HI/(HI+H₂) is not always a good enough parameter to describe the strength of the UV field.

4.2. The σ and ζ dichotomy: skin and flesh of clouds.

The difference in behaviour of the DIB strengths in different environments has led to the suggestion that only a few discrete sets of cloud properties exist, not a broad, continuous “spectrum” (Krelowski & Sneden, 1995). Only two major classes of clouds are said to exist, being the σ and ζ cloud type while two more apparent types seem to exist, the *CS* (*circumstellar*) and the *Orion* cloud types. The properties of these clouds are, as summarized in Krelowski & Sneden (1995), given in Table 4. Lines of sight with properties that are in between two types are then decomposed into σ and ζ components which has even led to the idea that the giant CO complex observed in Perseus (Per OB2 association) is in fact composed of two overlapping clouds, one σ and one ζ cloud (Krelowski et al. 1996). In the light of our ionization hypothesis we can now better understand what really happens.

Assuming that the DIB carrier behaviour reflects an ionization equilibrium, we can see from Fig. 2 that there is indeed a big difference in ionization potential for the $\lambda 5780$ and $\lambda 5797$ DIBs. The $\lambda 5797$ carrier is easily ionized, but is already largely destroyed when the $\lambda 5780$ reaches its maximum. In this point of view, ζ clouds are clouds where the local UV field is rather low, whereas σ type clouds suffer from a strong local UV field. Orion type clouds are, in the same line, environments characterized by extreme UV radiation. The differences in ionization potentials between the carriers of the $\lambda 5780$ and $\lambda 5797$ DIB thus easily explain DIB observations and ratios of those two DIBs towards σ and ζ clouds.

Cardelli (1988) notes that the total-to-selective extinction R_V can be used as a parameter to estimate the strength of the UV field. So ζ clouds have a low value for the R_V while the value increases for σ and *Orion* type clouds. Simple neutral molecules should be strong for weak UV fields, but easily destroyed for stronger UV-fields, which is again as observed.

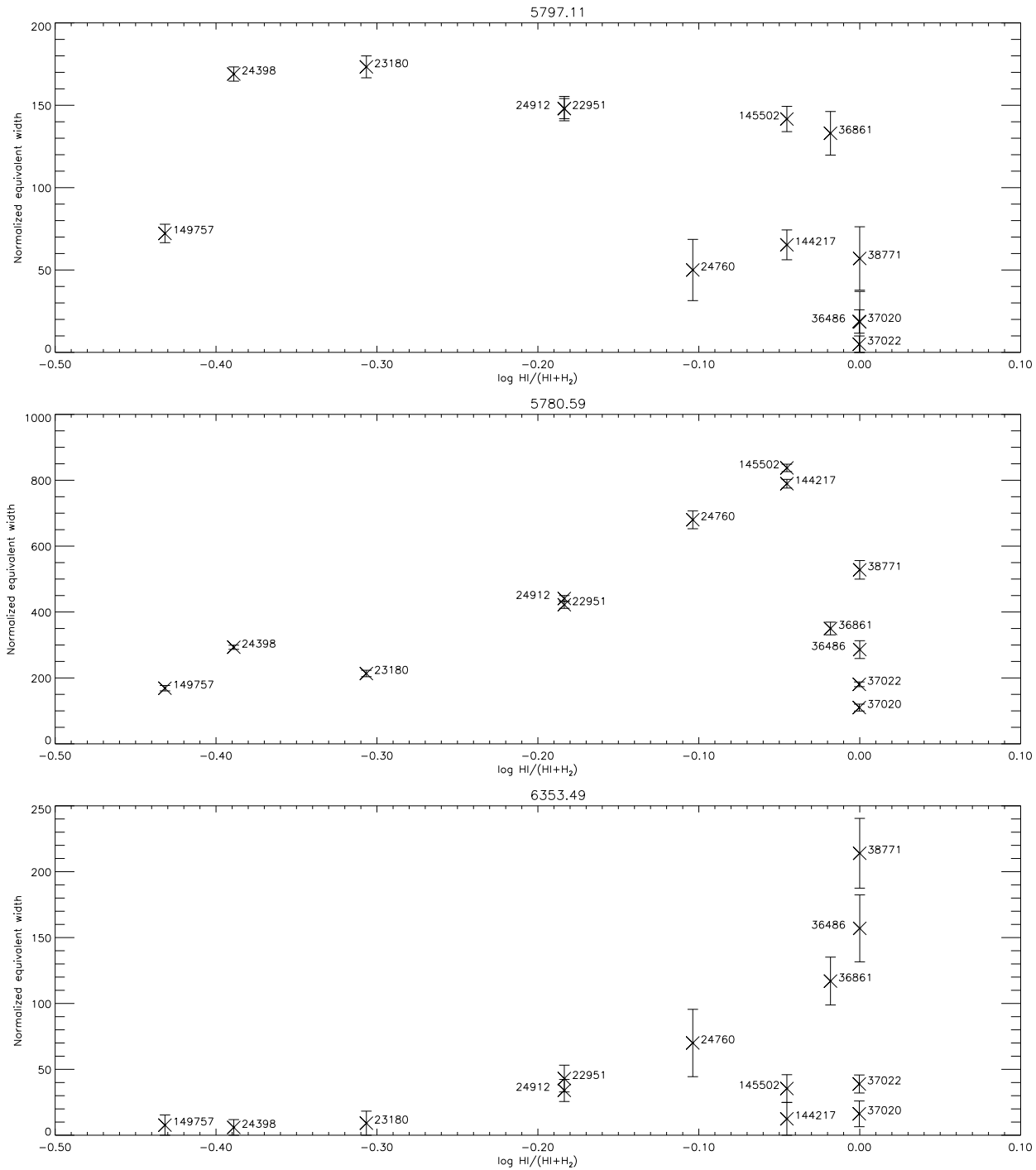


Fig. 2. The normalized equivalent widths as a function of the HI/(HI+H₂) column density ratio for the $\lambda\lambda 5797$ (top), 5780 (middle) and 6353 (bottom) DIB in the program stars. One notes a rise and fall of the DIB strength at different values of HI/(HI+H₂) indicating different photo-ionization and recombination properties.

The drastic changes in strength of the UV field are caused by the shielding from UV radiation by the outer layers of the clouds, the so-called “skin effect”. The more we look at the outer edges of clouds, the more we see UV-processed material. For this reason it is important to notice that a good estimate of

the local UV field from model calculations has to include the geometry of the cloud which may play a crucial role.

The σ/ζ dichotomy just expresses in fact the differences in physical condition between the outer skin and the inner flesh of clouds. It seems thus unnecessary and not very useful to decompose intermediate types of clouds into σ and ζ components;

Table 4. The division of clouds into families as summarized in Krelowski & Sneden (1995)

	ζ	σ	<i>Orion</i>	<i>CS</i>
$\lambda 5780$	comparable to $\lambda 5797$	very strong	weak but present	hardly visible
$\lambda 5797$	very deep	shallow	absent	hardly visible
Far-UV extinction	high	low	flat	gray
2200 Å bump	broad	narrow	very weak	absent
R_V	~ 3.1	~ 4.5	~ 5	hard to obtain
Simple molecules (CH, CN)	strong	below level of detection or very weak	not detected	not detected
Example	ζ Oph	σ Sco	HD37022	HD45725

those intermediate types just represent how much skin and flesh are crossed by the line-of-sight.

We end by noting that we did not explain the features for the *CS* type cloud. First of all, observations for this type of cloud are scarce and of insufficient quality. Moreover, observations are only carried out towards Be stars, where we can expect that the circumstellar abundance of carbon atoms that would compose the DIB carriers is rather low. This is also reflected by the complete absence of the 2200 Å feature. In that case we wouldn't expect to see DIBs. On the other hand, in the spectra of evolved carbon rich stars with a circumstellar shell (such as HD44179 and HR4049) carbon can be expected to be very abundant, but nevertheless no DIBs have been found so far except for the Red Rectangle (HD44179, see Scarrott et al. 1992). Probably the formation of the DIB carrier is a slow process or is critically determined by the surrounding temperature and density.

4.3. DIBs and UV extinction curve

Assuming now that the carrier molecules are large molecules like PAHs and fullerenes, we can also explain the UV extinction curves in different cloud conditions. Désert et al. (1995) considered independently the far-UV non-linear rise, the linear rise and the width and position of the 2200 Å bump in relation to DIB measurements, using the parametrization scheme of Fitzpatrick & Massa (1988). Their findings were (as summarized by Désert & Jenniskens, 1995):

- There is no linear correlation of DIB strength with linear rise or the ratio of total to selective extinction in the visual.
- The far-UV non-linear rise and bump width are clearly anti-correlated with the DIB strength
- A positive correlation with the 2175 Å bump does exist but is weaker

The far-UV non-linear rise absorption feature correlates with the abundance of molecular hydrogen (Jenniskens et al. 1992). This makes the possibility that the far-UV non-linear rise is caused by neutral molecules very likely. However, neutral PAHs of sizes less than about 60 carbon atoms have no strong absorptions in the visible and probably do not account for DIBs. Ionized PAHs do (see Salama et al. 1996 for a review). If DIBs are due to some ionized PAH species and the far-UV non-linear rise is due to neutral PAHs, a low degree of ionization will result in relatively weak DIBs and a large far-UV non-linear rise which is consistent with observations as stated in Table 4.

5. Conclusion

A consistent selected sample of 44 DIBs in the range from 4501-6811 Å has been measured towards single cloud stars representing very different environments. A study of mutual DIB correlations in these lines of sight has been performed and assessed. We do not find DIB pairs that perfectly correlate (within the confidence allowed by measurement and statistical analysis uncertainties). Some DIBs do indeed closely correlate with each other which may point to similarities of the carriers. Two isolated families of DIBs can be found with slightly opposite behaviour.

The behaviour of the DIBs with respect to the local UV field is investigated using the relative HI column density as a first estimate of the strength of the UV field. This leads to the hypothesis that most of the DIB carriers are undergoing photoionization. Differences between the behaviour of different DIBs is then interpreted as differences in ionization and recombination properties on molecular level. Lines of sight that are close to each other but have very different DIB strengths point to shielding of UV radiation in the flesh of clouds by their outer skin, the so-called “skin effect”. This means that also the geometry of the cloud has to be taken into account to have a good idea about the real situation.

Assuming also that the DIB carriers are large molecules based on carbon, this ionization hypothesis can also explain the classification of cloud conditions into ζ , σ and *Orion* types as a sequence in strength of the surrounding UV field.

The mutual DIB correlations, the variation with UV field and the link with UV extinction curves are consistent with the hypothesis of DIB carriers such as large carbonaceous molecules in neutral, anion or cation state.

Acknowledgements. We thank the staff of OHP for help during the observations. PE is a recipient of an APART fellowship.

References

- Baranne A., Queloz D., Mayor M. et al., 1996, *A&AS* 119, 373
- Cardelli J., 1988, *ApJ* 335, 177
- Chlewicki G., van der Zwet G.P., Van Ijzendoorn L.J., Greenberg J.M., 1986, *ApJ* 305, 455
- Code A.D., 1958, *PASP* 70, 407
- Désert F.-X., Jenniskens P., 1995, in “Diffuse Interstellar Bands”, eds. Tielens A.G.G.M. & Snow T.P., Kluwer Academic Publisher, 97
- Désert F.-X., Jenniskens P., Dennefeld M., 1995, *A&A*, 303, 223

- Fitzpatrick E.L., Massa D., 1988, ApJ, 328, 734
Ehrenfreund P., Foing B.H., d'Hendecourt L., Jenniskens P., Désert F.X., 1995, A&A 299, 213
Ehrenfreund P., Foing B.H., 1996, A&A, 307, L25
Foing B.H., Ehrenfreund P., 1994, Nature 369, 296
Foing B.H., Ehrenfreund P., 1997, A&A 317, L59
Herbig G.H., 1975, ApJ 196, 129
Herbig G.H., 1995, ARA&A 33, 19
Jenniskens P., Désert F.-X., 1994, A&AS 106, 39
Jenniskens P., Ehrenfreund P., Désert F.X., 1992, A&A 265, L1
Josafatsson K., Snow T.P., 1987, ApJ 319, 436
Kerr T.H., Hibbins R.E., Miles J.R., Fossey S.J., Sommerville W.B., Sarre P.J., 1996, MNRAS 283, L105
Krelowski J. & Sneden C., 1995, in "Diffuse Interstellar Bands", eds. A.G.G.M. Tielens & Snow, T.P., Kluwer Academic Publisher, 13
Krelowski J., Walker G.A.H., 1987, ApJ 312, 860
Krelowski J., Westerlund B.E., 1988, A&A, 190, 339
Krelowski J., Megier A., Strobel A., 1996, A&A 308,908
Merrill P.W., 1934, PASP 46, 206
Salama F., Bakes E.L.O., Allamandola L.J., Tielens A.G.G.M., 1996, ApJ 458, 621
Savage B.D., Drake J.F., Budich W., Bohlin R.C., 1977, ApJ 216, 291
Scarrott S.M., Watkin S., Miles J.R., Sarre P.J., 1992, MNRAS, 255, 11
Sonnentrucker P., Cami J., Foing B.H., Ehrenfreund P., 1997, submitted to A&A